ACS OMEGA

http://pubs.acs.org/journal/acsodf

Article

Fluorescent Carbon Dots Derived from Vehicle Exhaust Soot and Sensing of Tartrazine in Soft Drinks

Sekar Thulasi, Arunkumar Kathiravan, and Mariadoss Asha Jhonsi*

Cite This: *ACS Omega* 2020, 5, 7025−7031

Read Online

ACCESS | Metrics & More | Article Recommendations | Supporting Information

ABSTRACT: Recycling of waste into valuable products plays a significant role in sustainable development. Herein, we report the conversion of vehicle exhaust waste soot into water-soluble fluorescent carbon dots via a simple acid refluxion method. The obtained carbon dots were characterized using microscopic and spectroscopic techniques. Microscopic techniques reveal that the prepared carbon material is spherical in shape with an average particle size of ∼4 nm. Spectroscopic studies exhibited that the carbon dots are emissive in nature, and the emission is excitation-dependent. Further, the prepared carbon dots were successfully utilized as a fluorescent probe for the detection of tartrazine with a limit of detection of 26 nM. The sensitivity of carbon dots has also been realized by the detection of trace amounts of tartrazine in commercial soft drinks. Overall, this work demonstrates the conversion air pollutant soot into value-added fluorescent nanomaterials toward sensing applications.

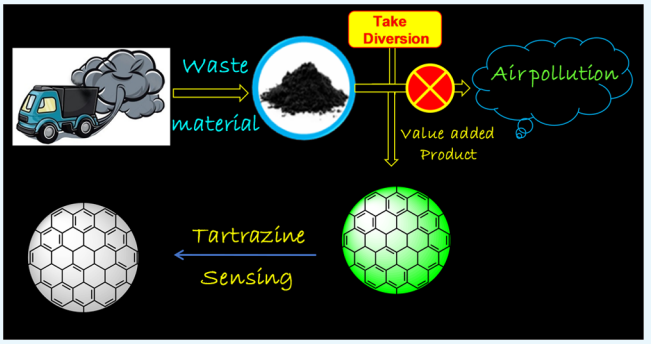

INTRODUCTION

Conversion of waste into a value-added material is a trend in research; owing to this leads sustainable development via recycling of used and unused scraps, especially soot waste.[1] Industries and vehicles exhaust pollutants, such as carbon monoxide, nitrogen oxide, particulate matter, ammonia, and sulfur dioxide, which impose many adverse effects on a living being.[2] In the present decade, we cannot completely avoid the usage of fuel in vehicles owing to the various hurdles on the 100% utilization of renewable energy resources. Among the various air pollutants, a vehicle exhaust soot emission consists of higher percentage of carbon with other elements like N and S from the source of fuel.[3] On the other side, researchers are looking for an invention of a novel, functionalized, and biocompatible nanomaterial for a wide range of applications.[4] The growing research areas such as bioimaging, biosensing, light-emitting diodes, etc. are consistently searching of a nanomaterial, which fits for the mentioned fields; especially in the past one decade, researchers are attracted by carbon-based nanomaterials owing to their specific properties of water solubility, fluorescence nature, photo and storage stability, biocompatibility, etc.[5−7] These urge the focused research on improving the efficiency of a fuel and conversion of pollutants into value-added products to maintain a sustainable environment.

Carbon dots (CDs) are widely used as an alternative for organic fluorophores and heavy metal-containing semiconductor quantum dots in biomedical, photovoltaic, and sensing applications as well as anti-icing/bioadhesor.[8−11] CDs are a new type of nanomaterial that consists of a graphitic core and an amorphous shell with an average particle size of less than 10 nm, which shows good water solubility, low toxicity, fluorescence property, and photostability.[12] It can be generated by various techniques such as electrochemical deposition,[13] microwave,[14] hydrothermal and solvothermal methods,[15] pyrolysis,[16] etc. Their surface is viable for modification by carbonyl, carboxylic, and amine functional groups, significantly making them as recognizable by enzymes in the organism. However, most of the reported CDs were derived from carbon-rich organic molecules like glucose, cellulose, and phenolic compounds[17−19] and biomass such as algal blooms,[20] coriander leaves,[21] lotus root,[22] radish,[23] ginger,[24] grass,[25] coffee bean shells,[26] chitosan[27] etc. Conversion of pollutants into value-added products like CDs using ultrasonication of food waste has been reported by Lee et al.[28] Similarly, conversion of soot collected from a burning candle,[29] tire soot,[30] and natural gas[31] into CDs and their biological applications have been reported.[32,33] Recently, we have also reported the fuel waste into fluorescent CDs for sensing applications.[34]

Received: February 17, 2020
Accepted: March 6, 2020
Published: March 18, 2020

https://dx.doi.org/10.1021/acsomega.0c00707
ACS Omega 2020, 5, 7025−7031

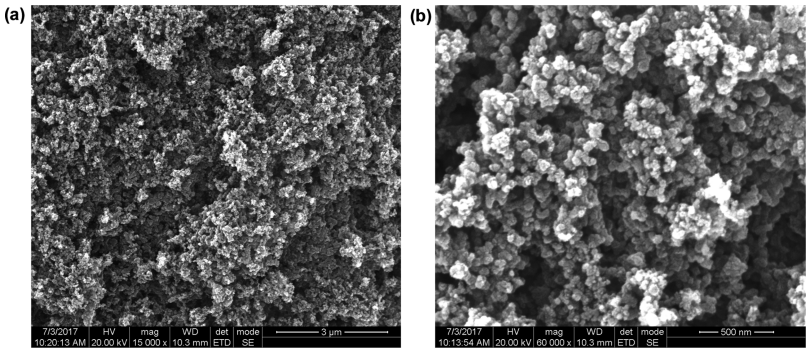

Figure 1. HR-SEM images of (a) soot and (b) CDs.

Food additives are used to improve the taste, quality, appearance, and other commercial requirements. Few types of food additives[35] are coloring agents (tartrazine and sunset yellow), flavor enhancers (monosodium glutamate commercially known as Ajinomoto), artificial sweetener (aspartame and acesulfame K), etc., which are commonly used in food and beverages. However, most human beings are allergic to such food additives, which cause many adverse health issues like hives or diarrhea, asthma, rhinitis and sinusitis, itching, rashes, and swelling.[36,37] For instance, a food colorant like tartrazine is an azo group dye molecule, whose limit of existence in the food content is fixed by the World Health Organization and the Food and Agricultural Organization, is 50 mg/kg. However, in most of the commercial food beverages as well as in the domestic preparations, the level of the coloring agent is not measured according to the WHO report, which may cause[38] few of the abovementioned negative effects. Hence, the detection of tartrazine has gained significance, and a few related reports could be found in the literature.[39] Aloe-derived carbon dots were used to detect tartrazine in a food sample.[40] Yuan et al. detected a well-known food colorant, sunset yellow, from the analysis of soft drinks with a satisfactory result by means of fluorescent CDs.[41] Even though a number of methods and materials are available for the detection of food additives, the high cost, tedious procedures, difficulty in synthesis, etc. motivate us to bring a simple, sensitive, and cost-effective material for the same matter.

In this work, the conversion of pollutant (exhaust soot derived from a diesel-fueled lorry) into a value-added product (CDs) is reported via the facile one-step acid refluxion method. The fluorescence nature of the CDs has been effectively used as a probe for the detection of tartrazine. The detection was extended in commercially available soft drinks.

RESULTS AND DISCUSSION

Synthesis of Carbon Dots. Carbon dots were synthesized from a vehicle exhaust soot by a one-pot acid refluxion method using nitric acid.[42] In brief, the soot was collected from a diesel engine lorry exhaust pipeline. The collected soot (1 g) was mixed with 200 mL of 5 M nitric acid, and the mixture was refluxed at 100 °C for 12 h. Consequently, the reflexed mixture was kept aside without disturbance to cool down to room temperature naturally. It is observed that the reaction mixture was turned to a reddish brown color with black precipitate deposition at the bottom. Furthermore, the solution mixture was centrifuged at 5000 rpm for 30 min to separate the bulkier carbon particles and unreacted soot material, which yields clear reddish brown color carbon dots. The brown fluorescent supernatant was collected, neutralized with sodium carbonate, and filtered via a 0.22 μm membrane filter (cellulose) to remove more than micrometer-sized particles and unreacted materials. Following that, the solution was dialyzed using a dialysis membrane bag (1000 MWCO) for 32 h. This process is essential to remove the less than nanometer-sized particles, small molecules, and removal of excess salt to derive the pure carbon dots (dialysis water is changed every 6 h). The clear dark brown solution was collected, and the volume was reduced via vacuum distillation and dried in a vacuum oven. Finally, dried fluorescent carbon dots were collected (55% product yield) and stored at room temperature.

Surface Characterization. The SEM images of collected soot and the derived CDs are given in Figure 1a,b, respectively, and the elemental composition details with the EDAX spectrum is shown in Figure S1. The SEM analysis clearly illustrates that the waste soot particles are rich in carbon (85.45%) and oxygen (14.54%), and the CDs derived from the soot after acid refluxion consist of aggregates of carbon nanoparticles, having nearly spherical morphology with relatively regular size and homogeneity. The EDAX data analysis exposes that CDs mainly consists of C (26.9%) and O (42.7%), which demonstrates that CDs are made up of an oxygenous carbon structure. Other elements also present in trace amounts may originate from the precursor soot. The powder XRD pattern of carbon dots is shown in Figure 2, which exhibits a sharp diffraction peak at 2θ = 29° and also many small diffraction peaks at 2θ = 32, 35, 38, 42, and 48°. It indicates that the carbon atoms are arranged in a considerably

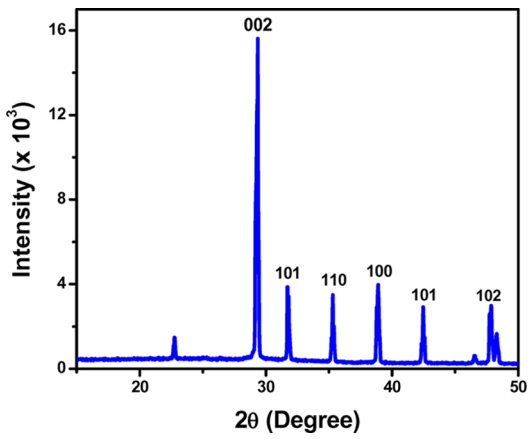

Figure 2. Powder XRD pattern of CDs.

https://dx.doi.org/10.1021/acsomega.0c00707
ACS Omega 2020, 5, 7025−7031

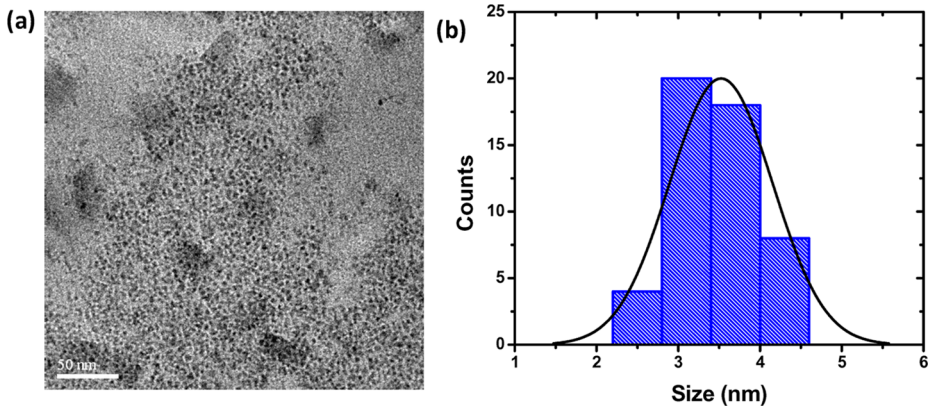

Figure 3. (a) HR-TEM image (50 nm scale) and (b) histogram plot of CDs.

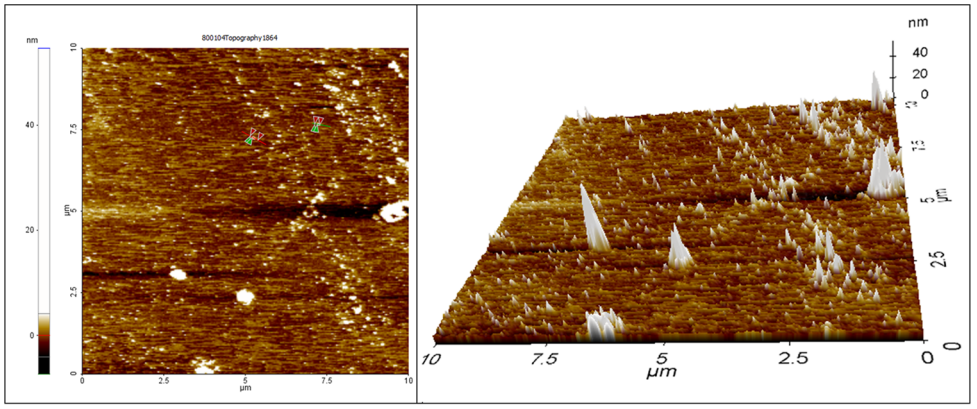

Figure 4. Atomic force microscopy image of CDs in a 10 μm scale (right-hand side) and the same in a three-dimensional view (left-hand side).

unsystematic manner as well as an amorphous nature induced by more oxygen-containing groups on the surface of CDs. Figure 3a shows the TEM image and histogram of CDs, and it reveals that the particles are quasi-spherical in shape with a nanometer size. The average particle size of CDs is in the range of 3−4 nm, and the size distribution is displayed in the histogram plot (Figure 3b). Figure 4 shows the AFM image of the derived CDs, and it exposes that most of the particles are spherical-shaped and well dispersed. The height profile (Figure S2) indicates the maximum of 6 nm of size from the surface, and the surface looks quite smooth, which confirms the uniform distribution of the particles on the surface. The particles size derived from TEM and AFM are consistent with each other, and both characterizations confirm that the prepared CDs are nanometer-sized particles.

The FT-IR analysis of the prepared CDs is shown in Figure 5a, which portrays that the presence of peak positions at 1795 and 3410 cm^{-1} were associated with the stretching vibrations of carbonyl (C═O) and hydroxyl (−OH) groups, respectively. The characteristic peaks at 1330 and 829 cm^{-1} were due to the stretching vibrations of sp^2 and sp^3 C−H, and the peak located at 1593 cm^{-1} corresponds to the C═C stretching vibration. The 2437 cm^{-1} peak is assigned for NO_3^- stretching vibration. The FT-IR data revealed the formation of unsaturated carbon during the carbonization process and the presence of rich oxygen-containing groups (carboxyl, carbonyl, and hydroxyl) on the surface of CDs. Raman analysis (Figure S3) exposed that the appearance of D and G bands of the prepared CDs were at 1351 and 1552 cm^{-1}, respectively. The existence of D and G bands illustrate the confirmation of sp^3-

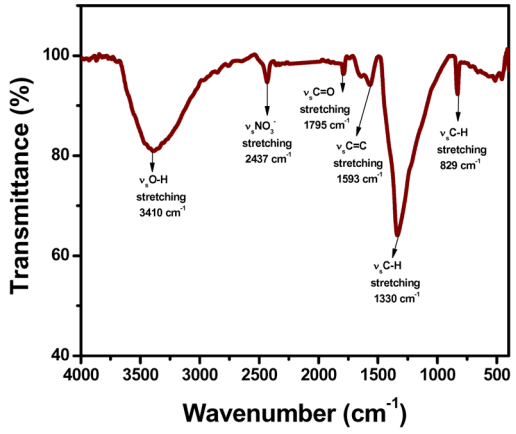

Figure 5. FT-IR spectrum of CDs.

hybridized amorphous carbon particles and the ε_{2g} mode of sp^2-hybridized graphitic carbon atoms, respectively. Further, the ratio of I_D/I_G of 1.01 clearly represents the prepared CDs consisting of a nanocrystalline graphitic core surrounded by a disorder/amorphous shell. The proton NMR analysis of CDs is shown in Figure S4, which reveals that the sp^3 C−H proton is present at the region 1−2 ppm, carbonyl, hydroxyl, and ether protons are present at 3−4 pm, and the aromatic sp^2 and aldehyde proton is an occurrence in the region 7−9 ppm. The solid-state ^{13}C NMR spectrum is shown in Figure S5, and the signal at 190 ppm was assigned to carboxyl carbon (COO−), while the signal at 125 ppm was designated to aromatic carbons. Further, the signal around 97 ppm is for carbonyl

https://dx.doi.org/10.1021/acsomega.0c00707
ACS Omega 2020, 5, 7025−7031

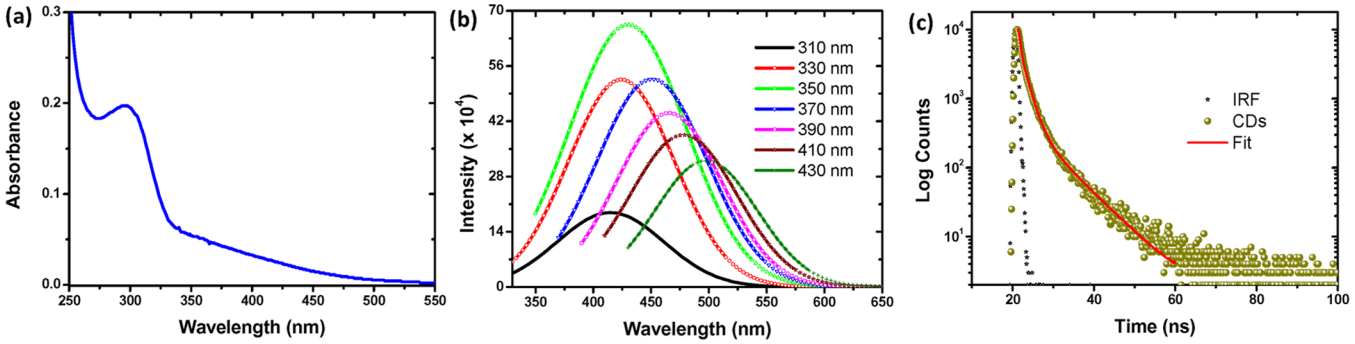

Figure 6. (a) UV−visible absorption, (b) corrected emission spectra at different excitation wavelengths, and (c) time-resolved fluorescence decay (λ_{exi} = 360 nm) of CDs.

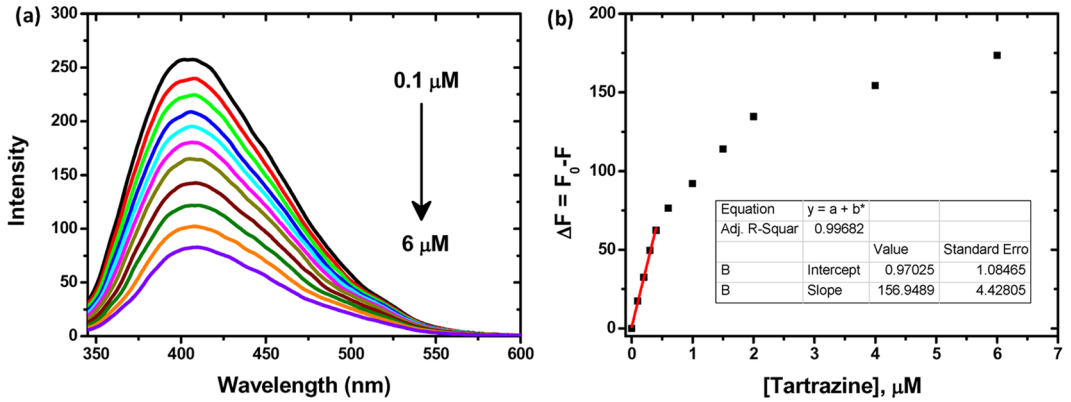

Figure 7. (a) Fluorescence quenching study of CDs in the absence and presence of various concentrations of tartrazine (0.1−6 μM) in water. (b) Detection limit plot.

carbons (C−O), and the signal in the range of 6−50 ppm was assigned to carbon bonded with hydrogen or other carbons. Zeta potential measurement exposed that CDs are negatively charged with a value of −0.2 mV, which specifies the presence of a negatively charged functional group on the surface of CDs and the surface is the hydrophilic nature. This imparts the high solubility of CDs in water. Further, the nature of bonding on the surface of CDs is characterized by the X-ray photoelectron spectroscopy technique and is shown in Figure S6a. The survey spectrum represented the presence of C, O, N, and Na (285, 530, 407, and 497 eV) elements. Nitrogen and sodium ions originated from the oxidative acid treatment and neutralization process. Hence, our interest is to analyze the carbon and oxygen bonding nature on the surface of CDs. So, the deconvoluted spectra of C 1s and O 1s were thoroughly examined and presented in Figure S6b,c. In the C 1s deconvoluted spectrum, the derivative peaks at 282.9, 284.5, and 287.9 eV were assigned to −C−C−, −C═C/C−N, and C═O, respectively. Similarly, the peaks located in the O 1s deconvoluted spectrum at 531.3, 533.3, and 536.1 eV were designated to the bonding of −C═O, −C−OH, and −C−O−C−, respectively. From the results of NMR, FT-IR, and XPS measurements, we have visualized the structure of the prepared material (CDs), which consists of various functional moieties and bonding nature on its surface.

Photophysical Characterization and Fluorescence Stability Studies. The UV−visible absorption spectrum of CDs is shown in Figure 6a, and it exhibits a sharp peak at 295 nm, which corresponds to $\pi-\pi^*$ transitions in the aromatic C═C bond in the carbon core. A broad shoulder in the region of 330−450 nm is due to $n-\pi^*$ transitions in the C═O bond, which originates from the surface functional groups of CDs. As similar to the reported carbon dots, the prepared CDs also exhibit the excitation-dependent emissive property (Figure 6b). The emission maximum is centered at 425 nm at an excitation of 360 nm. The origin of the fluorescence property of the derived CDs may arise from the various defects present on the surface of CDs.[34] Further, the fluorescence decay of carbon dots shown in Figure 6c is fitted by a multiexponential function $[F(t) = A_1 \exp(-t/\tau 1) + A_2 \exp(-t/\tau_2) + A_3 \exp(-t/\tau_3)]$ with the lifetimes of τ_1 = 0.56 ns (18%), τ_2 = 1.78 ns (35%), and τ_3 = 5.21 ns (47%), and the average lifetime is calculated as τ_{avg} = 3.17 ns. The multiple lifetimes of CDs are due to a wide range of chemical environments on the surface of CDs.[43] The quantum yield (φ) of CDs is determined using quinine sulfate as a reference.[44] For the measurement of φ, the optical density of CDs in water (η = 1.33) was fixed to 0.1 at a wavelength of 366 nm. Fluorescence quantum yield (ϕ_F) for CDs was calculated by using eq 1

$$\phi_F = (A_R/A_S)\,(I_S/I_R)\,(\eta_S/\eta_R)^2\,\phi_R \rightarrow \quad (1)$$

where the subscript "S" refers to the samples, the subscript "R" refers to quinine sulfate, A is the absorbance at the excitation wavelength, I is the integrated emission area, and η is the solvent refraction index. The quantum yield for CDs is found to be 3%, which is good enough for various sensing applications.

Further, it is necessary to analyze fluorescence stability of CDs for versatile applications. The stability is investigated under four different parameters such as storage time, pH, light irradiation, and ionic strength. The detailed results are

https://dx.doi.org/10.1021/acsomega.0c00707
ACS Omega 2020, 5, 7025−7031

depicted in Figure S7, which explores that the fluorescence property of CDs remains stable for up to 90 days. It shows a higher fluorescence nature at the neutral pH, and there was a pH-dependent fluorescence behavior. Optimum fluorescence behavior in the pH range of 4−9 and lower of higher of that leads to diminishing in fluorescence ability. Photostability of CDs is checked by UV light irradiation for a period of 2 h, and the quite stable nature of CDs is found. The effect of ionic strength is checked with addition of maximum of 1 M NaCl in CDs, and it is observed that there is not much variation in the fluorescence property in the presence of NaCl. So, the prepared CDs exhibit stability in different environments, which may extend its utilization in biological fields.

Sensing of Tartrazine. Tartrazine is one of the most widely used food coloring agents, and its excess limit in food may cause allergic symptoms to human beings. So, it is essential to detect tartrazine in food samples. For this purpose, we have adopted a highly sensitive and simple analytical methodology, namely, the fluorescence quenching technique. The fluorescence quenching measurements of CDs in the presence of various concentrations of tartrazine (0.1−6 μM) were conducted, and the spectrum is displayed in Figure 7a. Upon increasing the concentration of tartrazine, the fluorescence intensity of CDs is found to regularly decrease. The sensitivity of CDs is estimated from the slope of the plot (Figure 7b) between the relative change ($\Delta F = F_0 - F$) in fluorescence intensity and tartrazine concentration. For tartrazine concentration in the range from 0.1 to 0.5 μM, the plot showed an excellent linear trend with a slope of 1.56×10^8 M^{-1} and the LOD was calculated to be 26 nM. The mechanism of fluorescence quenching of CDs by tartrazine may either be due to the excited state energy transfer or inner filter effect. Since both the CDs and tartrazine exhibit absorption in the same region, the most possible quenching mechanism is the inner filter effect. A similar type of sensing mechanism was proposed in the literature.[45] The time-resolved fluorescence technique is employed to understand the sensing mechanism. Figure S8 shows the fluorescence decay of CDs and with tartrazine. As expected, the fluorescence decay is not altered even in the presence of the highest concentration of tartrazine; thus, the quenching type is static with an inner filter effect.

Since the possibility of occurrence of few metal ions in food products along with coloring agents is high, it is essential to study the interference of metal ions at the same time as sensing of tartrazine. To understand the role of metal ions on the fluorescence quenching of CDs by tartrazine, we have conducted the interference studies with various metal ions. CDs were exposed to various metal ions (1 μM), and fluorescence spectra were recorded. Surprisingly, the Fe^{3+} ion quenches the fluorescence of CDs predominantly. Figure 8 shows the selectivity plot of CDs with metal ions. Further, to quantify Fe^{3+} ion sensing, the fluorescence spectrum of CDs was recorded as a function of Fe^{3+} ion, as shown. The fluorescence spectrum of CDs was gradually decreased with the increasing concentration of Fe^{3+} ion (Figure S9a). The limit of detection of the Fe^{3+} ion was calculated using the three (σ/slope) relations. The linearity was observed for the plot of fluorescence intensity change against the lower concentration of Fe^{3+} ion (Figure S9b). The lowest detection limit was determined to be 13 nM. A combined XPS and FT-IR result indicated that there are carboxyl, hydroxyl, and amine functional groups on the surface of the as-synthesized CDs.

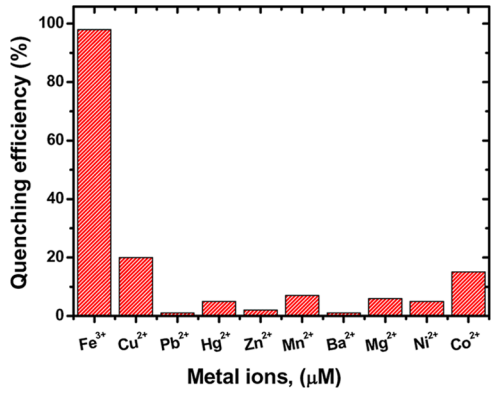

Figure 8. Selectivity plot of CDs with various metal ions (1 μM).

Therefore, it could be inferred that CDs can form complex with Fe^{3+} ions through such functional groups, resulting in fluorescence quenching with high selectivity/sensitivity. Similar reports are available in the literature.[46−48]

Intriguingly, both tartrazine and Fe^{3+} ion quench the CD fluorescence with LOD values of 26 and 13 nM, respectively. In this higher sensitivity, it is very difficult to distinguish the one that quenches the fluorescence of CDs. To get rid of the mentioned issue, we are giving remedy for sensitive detection of tartrazine even if Fe^{3+} ions persist in the solution. Based on our experimental observations, the selective sensing of tartrazine could be achieved by the addition of 1 mM potassium thiocyanate to solution mixtures. Since Fe^{3+} can readily complex with potassium thiocyanate and it is not free to quench the fluorescence of CDs, in this way, one can qualitatively detect the tartrazine in the mixture. The effect of interference of other food additives, such as monosodium glutamate (flavor enhancer) and acesulfame K (artificial sugar) has also been investigated, and the results are shown in Figure S10. The fluorescence of CDs is not quenched by both monosodium glutamate and acesulfame K. However, in the presence of tartrazine, the strong quenching was observed. Hence, the prepared CDs are prospective materials for the detection of tartrazine even with other food additives.

Detection in Soft Drinks. The prepared fluorescent CDs were employed to detect the trace level of tartrazine in various soft drink samples. The results of the pretreated soft drinks spiked with known concentrations of tartrazine are shown in Table 1. The excellent recoveries ranging from 87 to 100.6% were attained. These results signify the accuracy and reliability of the prepared CDs toward the determination of tartrazine in commercial soft drinks.

Table 1. Recovery of Tartrazine Spiked with Different Soft Drinks by CDs

soft drinks	added (μM)	found (μM)	recovery (%)
sample I	0.1	0.0991	99.18
	0.2	0.2012	100.61
	0.4	0.3994	99.85
sample II	0.1	0.1008	100.87
	0.2	0.1980	99.02
	0.4	0.4012	100.3
sample III	0.1	0.0870	87
	0.2	0.1997	99.87
	0.4	0.3922	98.06

https://dx.doi.org/10.1021/acsomega.0c00707
ACS Omega 2020, 5, 7025−7031

CONCLUSIONS

In summary, successful conversion of waste soot into fluorescent CDs by a simple one-pot method is demonstrated. The fluorescence property of the derived CDs was effectively used to detect tartrazine through a turn-off fluorescence method. Further, this method is successfully employed to detect tartrazine in soft drinks. Thus, the prepared CDs could be used for selective and sensitive determination of tartrazine in foodstuff products. Overall, this work demonstrated the conversion of a vehicle soot to a value-added product and the same has been successfully utilized for sensing applications.

EXPERIMENTAL SECTION

Materials and Methods. Waste soot was collected from a diesel engine lorry exhaust pipeline. Ultrapure water was used for the synthesis of carbon dots and all measurements. A dialysis membrane bag was purchased from HiMedia, and a dialysis tube Float-A-Lyzer was purchased from Synergy Scientific Services. Tartrazine was purchased from Sigma-Aldrich and used as such without further purification. Monosodium glutamate and acesulfame K were procured from TCL chemicals. The commercial coloring agent (Kesari powder) was purchased from a nearby provisional store.

The particle size and morphology of the synthesized CDs were investigated by high-resolution transmission electron microscopy (HRTEM; JEOL JEM-2100; with an accelerating voltage of 120 kV). The TEM specimen was prepared by dropping a diluted CD solution onto a carbon-coated copper grid followed by the evaporation of the water solvent. SEM measurement and EDAX analysis were done by using Nova NANO SEM 600 from FEI Company, Netherlands. The FT-IR spectrum was recorded by using a JASCO FT-IR ATR 6300 spectrometer at room temperature in the range of 4000−400 cm^{-1}. ^{1}H NMR (500 MHz) and ^{13}C NMR (125, 100 MHz) spectra of CDs were recorded on a Bruker NMR spectrometer in D_2O with tetramethylsilane (TMS) as an internal standard. Topographic analysis is done with Park Systems (XE-100 AFM) for an area of 10 × 10 μm scale with a resolution of <1.5 nm. Absorption spectra were recorded using a PerkinElmer Lamda 25 UV−visible spectrophotometer. The fluorescence quenching measurements were carried out with an Hitachi-made fluorescence spectrometer (model: F-4500). Time-resolved fluorescence decays were obtained by the time-correlated single photon counting (TCSPC) technique, exciting the sample at a 360 nm LED source. Data analysis was carried out by the software provided by IBH (DAS-6), which is based on deconvolution techniques using the nonlinear least squares method, and the quality of the fit is ascertained with a value of χ^2 < 1.1.

Sensing of Tartrazine in Soft Drinks. The soft drink samples were procured from a local superstore and used as is. In a typical assay, 0.3 mL of CDs is added to 2.7 mL of soft drinks in a cuvette and fluorescence was recorded. Further, the tartrazine solution (up to 30 μL; the maximum concentration of tartrazine is 6 μM) was gradually added into the CD solution and the solution was mixed well prior to the fluorescence spectrum being recorded.

ASSOCIATED CONTENT

Supporting Information

The Supporting Information is available free of charge at https://pubs.acs.org/doi/10.1021/acsomega.0c00707.

NMR, RAMAN, XPS, EDAX, AFM, and additional figures (PDF)

AUTHOR INFORMATION

Corresponding Author

Mariadoss Asha Jhonsi − *Department of Chemistry, B. S. Abdur Rahman Crescent Institute of Science and Technology, Chennai 600048, Tamil Nadu, India;* orcid.org/0000-0001-9071-8670; Email: jhonsiasha@gmail.com

Authors

Sekar Thulasi − *Department of Chemistry, B. S. Abdur Rahman Crescent Institute of Science and Technology, Chennai 600048, Tamil Nadu, India*

Arunkumar Kathiravan − *Vel Tech Research Park, Vel Tech Rangarajan Dr Sagunthala R&D Institute of Science and Technology, Chennai 600062, Tamil Nadu, India;* orcid.org/0000-0001-6131-460X

Complete contact information is available at: https://pubs.acs.org/10.1021/acsomega.0c00707

Notes

The authors declare no competing financial interest.

ACKNOWLEDGMENTS

S.T. thanks the department of chemistry and BSACIST for providing the lab facilities. M.A.J. acknowledges SERB for the TARE project (ref: TAR/2018/00048, Dt: 18.02.2019). The authors also acknowledge Mr. V. Srinivasan and Ms. S. Jayamatha SAB for the benchmark experiments.

REFERENCES

(1) Mulay, M. R.; Chauhan, A.; Patel, S.; Balakrishnan, V.; Halder, A.; Vaish, R. Candle soot: Journey from a pollutant to a functional material. *Carbon* **2019**, *144*, 684−712.

(2) Hardy, J. T. *Climate change: causes, effects, and solutions*; John Wiley & Sons: 2003.

(3) Devi, S.; Gupta, R. K.; Paul, A. K.; Kumar, V.; Sachdev, A.; Gopinath, P.; Tyagi, S. Ethylenediamine mediated luminescence enhancement of pollutant derivatized carbon quantum dots for intracellular trinitrotoluene detection: Soot to shine. *RSC Adv.* **2018**, *8*, 32684−32694.

(4) Khan, I.; Saeed, K.; Khan, I. Nanoparticles: Properties, applications and toxicities. *Arab. J. Chem.* **2019**, *12*, 908−931.

(5) Patel, K. D.; Singh, R. K.; Kim, H. W. Carbon-based nanomaterials as an emerging platform for theranostics. *Mater. Horiz.* **2019**, *6*, 434−469.

(6) Yuan, T.; Meng, T.; He, P.; Shi, Y.; Li, Y.; Li, X.; Fan, L.; Yang, S. Carbon quantum dots: An emerging material for optoelectronic applications. *J. Mater. Chem. C* **2019**, *7*, 6820−6835.

(7) Campuzano, S.; Yáñez-Sedeño, P.; Pingarrón, J. M. Carbon dots and graphene quantum dots in electrochemical biosensing. *Nanomaterials* **2019**, *9*, 1−18.

(8) Zhang, J.; Yu, S. H. Carbon dots: large-scale synthesis, sensing and bioimaging. *Mater. Today* **2016**, *19*, 382−393.

(9) Molaei, M. J. Carbon quantum dots and their biomedical and therapeutic applications: A review. *RSC Adv.* **2019**, *9*, 6460−6481.

(10) Esmeryan, K. D.; Castano, C. E.; Chaushev, T. A.; Mohammadi, R.; Vladkova, T. G. Silver-doped superhydrophobic carbon soot coatings with enhanced wear resistance and anti-microbial performance. *Colloids Surf., A* **2019**, *582*, 123880.

(11) Esmeryan, K. D.; Stamenov, G. S.; Chaushev, T. A. An innovative approach for in-situ detection of postejaculatory semen coagulation and liquefaction using superhydrophobic soot coated quartz crystal microbalances. *Sens. Actuators, A* **2019**, *297*, 111532.

(12) Lim, S. Y.; Shen, W.; Gao, Z. Carbon quantum dots and their applications. *Chem. Soc. Rev.* **2015**, *44*, 362−381.
(13) Wang, Y.; Wang, X.; Geng, Z.; Xiong, Y.; Wu, W.; Chen, Y. Electrodeposition of a carbon dots/chitosan composite produced by a simple in situ method and electrically controlled release of carbon dots. *J. Mater. Chem. B* **2015**, *3*, 7511−7517.
(14) De Medeiros, T. V.; Manioudakis, J.; Noun, F.; Macairan, J. R.; Victoria, F.; Naccache, R. Microwave-assisted synthesis of carbon dots and their applications. *J. Mater. Chem. C* **2019**, *7*, 7175−7195.
(15) Sahu, S.; Behera, B.; Maiti, T. K.; Mohapatra, S. Simple one-step synthesis of highly luminescent carbon dots from orange juice: Application as excellent bio-imaging agents. *Chem. Commun.* **2012**, *48*, 8835−8837.
(16) Lai, C. W.; Hsiao, Y. H.; Peng, Y. K.; Chou, P. T. Facile synthesis of highly emissive carbon dots from pyrolysis of glycerol; gram scale production of carbon dots/mSiO2 for cell imaging and drug release. *J. Mater. Chem.* **2012**, *22*, 14403−14409.
(17) Hill, S.; Galan, M. C. Fluorescent carbon dots from mono- and polysaccharides: Synthesis, properties and applications. *Beilstein J. Org. Chem.* **2017**, *13*, 675−693.
(18) Wu, P.; Li, W.; Wu, Q.; Liu, Y.; Liu, S. Hydrothermal synthesis of nitrogen-doped carbon quantum dots from microcrystalline cellulose for the detection of Fe^{3+} ions in an acidic environment. *RSC Adv.* **2017**, *7*, 44144−44153.
(19) Liu, Q.; Li, D.; Zhu, Z.; Yu, S.; Zhang, Y.; Yu, D.; Jiang, Y. N-doped carbon dots from phenol derivatives for excellent colour rendering WLEDs. *RSC Adv.* **2018**, *8*, 4850−4856.
(20) Zhu, L.; Yin, Y.; Wang, C. F.; Chen, S. Plant leaf-derived fluorescent carbon dots for sensing, patterning and coding. *J. Mater. Chem. C* **2013**, *1*, 4925−4932.
(21) Sachdev, A.; Gopinath, P. Green synthesis of multifunctional carbon dots from coriander leaves and their potential application as antioxidants, sensors and bioimaging agents. *Analyst* **2015**, *140*, 4260−4269.
(22) Gu, D.; Shang, S.; Yu, Q.; Shen, J. Green synthesis of nitrogen-doped carbon dots from lotus root for Hg(II) ions detection and cell imaging. *Appl. Surf. Sci.* **2016**, *390*, 38−42.
(23) Liu, W.; Diao, H.; Chang, H.; Wang, H.; Li, T.; Wei, W. Green synthesis of carbon dots from rose-heart radish and application for Fe^{3+} detection and cell imaging. *Sens. Actuators, B Chem.* **2017**, *241*, 190−198.
(24) Li, C. L.; Ou, C. M.; Huang, C. C.; Wu, W. C.; Chen, Y. P.; Lin, T. E.; Ho, L. C.; Wang, C. W.; Shih, C. C.; Zhou, H. C.; Lee, Y. C.; Tzeng, W. F.; Chiou, T. J.; Chu, S. T.; Cang, J.; Chang, H. T. Carbon dots prepared from ginger exhibiting efficient inhibition of human hepatocellular carcinoma cells. *J. Mater. Chem. B* **2014**, *2*, 4564−4571.
(25) Sabet, M.; Mahdavi, K. Green synthesis of high photo-luminescence nitrogen-doped carbon quantum dots from grass via a simple hydrothermal method for removing organic and inorganic water pollutions. *Appl. Surf. Sci.* **2019**, *463*, 283−291.
(26) Zhang, X.; Wang, H.; Ma, C.; Niu, N.; Chen, Z.; Liu, S.; Li, J.; Li, S. Seeking value from biomass materials: Preparation of coffee bean shell-derived fluorescent carbon dots via molecular aggregation for antioxidation and bioimaging applications. *Mater. Chem. Front.* **2018**, *2*, 1269−1275.
(27) Song, J.; Zhao, L.; Wang, Y.; Xue, Y.; Deng, Y.; Zhao, X.; Li, Q. Carbon quantum dots prepared with chitosan for synthesis of CQDS/auNPs for iodine ions detection. *Nanomaterials* **2018**, *8*, 1043.
(28) Park, S. Y.; Lee, H. U.; Park, E. S.; Lee, S. C.; Lee, J. W.; Jeong, S. W.; Kim, C. H.; Lee, Y. C.; Huh, Y. S.; Lee, J. Photoluminescent green carbon nanodots from food-waste-derived sources: Large-scale synthesis, properties, and biomedical applications. *ACS Appl. Mater. Interfaces* **2014**, *6*, 3365−3370.
(29) Pankaj, A.; Tewari, K.; Singh, S.; Singh, S. P. Waste candle soot derived nitrogen doped carbon dots based fluorescent sensor probe: An efficient and inexpensive route to determine Hg(II) and Fe(III) from water. *J. Environ. Chem. Eng.* **2018**, *6*, 5561−5569.
(30) Ko, H. Y.; Chang, Y. W.; Paramasivam, G.; Jeong, M. S.; Cho, S.; Kim, S. In vivo imaging of tumour bearing near-infrared fluorescence-emitting carbon nanodots derived from tire soot. *Chem. Commun.* **2013**, *49*, 10290−10292.
(31) Tian, L.; Ghosh, D.; Chen, W.; Pradhan, S.; Chang, X.; Chen, S. Nanosized carbon particles from natural gas soot. *Chem. Mater.* **2009**, *21*, 2803−2809.
(32) Liu, H.; Ye, T.; Mao, C. Fluorescent Carbon Nanoparticles Derived from Candle Soot. *Angew. Chem., Int. Ed.* **2007**, *46*, 6473−6475.
(33) Yang, S.-T.; Cao, L.; Luo, P. G.; Lu, F.; Wang, X.; Wang, H.; Meziani, M. J.; Liu, Y.; Qi, G.; Sun, Y.-P. Carbon Dots for Optical Imaging in Vivo. *J. Am. Chem. Soc.* **2009**, *131*, 11308−11309.
(34) Venkatesan, S.; Asha Jhonsi, M.; Kathiravan, A.; Muthupandian, A. Fuel waste to fluorescent carbon dots and its multifarious applications. *Sens. Actuators, B Chem.* **2019**, *282*, 972−983.
(35) https://www.who.int/news-room/fact-sheets/detail/food-additives
(36) *Food safety and standards authority of India ministry of and family welfare gov.* of India, New Delhi, lab manual, 2015.
(37) Celik Ertuğrul, D. FoodWiki: a Mobile App Examines Side Effects of Food Additives Via Semantic Web. *J. Med. Syst.* **2016**, *40*, 1−15.
(38) Downham, A.; Collins, P. Colouring our foods in the last and next millen nium. *Int. J. Food Sci. Technol.* **2000**, *35*, 5−22.
(39) Huang, S. T.; Shi, Y.; Li, N. B.; Luo, H. Q. Sensitive turn-on fluorescent detection of tartrazine based on fluorescence resonance energy transfer. *Chem. Commun.* **2012**, *48*, 747−749.
(40) Xu, H.; Yang, X.; Li, G.; Zhao, C.; Liao, X. Green Synthesis of Fluorescent Carbon Dots for Selective Detection of Tartrazine in Food Samples. *J. Agric. Food Chem.* **2015**, *63*, 6707−6714.
(41) Yuan, Y.; Zhao, X.; Qiao, M.; Zhu, J.; Liu, S.; Yang, J.; Hu, X. Determination of sunset yellow in soft drinks based on fluorescence quenching of carbon dots. *Spectrochim. Acta Part A Mol. Biomol. Spectrosc.* **2016**, *167*, 106−110.
(42) Wang, Q.; Zhang, S.; Ge, H.; Tian, G.; Cao, N.; Li, Y. A fluorescent turn-off/on method based on carbon dots as fluorescent probes for the sensitive determination of Pb^{2+} and pyrophosphate in an aqueous solution. *Sens. Actuators, B Chem.* **2015**, *207*, 25−33.
(43) Srinivasan, V.; Asha Jhonsi, M.; Kathiresan, M.; Kathiravan, A. Nanostructured Graphene Oxide Dots: Synthesis, Characterization, Photoinduced Electron Transfer Studies, and Detection of Explosives/Biomolecules. *ACS Omega* **2018**, *3*, 9096−9104.
(44) Adams, M. J.; Highfield, J. G.; Kirkbright, G. F. Determination of absolute fluorescence quantum efficiency of quinine bisulfate in aqueous medium by optoacoustic spectrometry. *Anal. Chem.* **1977**, *49*, 1850−1852.
(45) Wang, Y.; Mu, Y.; Hu, J.; Zhuang, Q.; Ni, Y. Rapid, one-pot, protein-mediated green synthesis of water-soluble fluorescent nickel nanoclusters for sensitive and selective detection of tartrazine. *Spectrochim. Acta. A* **2019**, *214*, 445−450.
(46) Chen, J.; Li, Y.; Lv, K.; Zhong, W.; Wang, H.; Wu, Z.; Yi, P.; Jang, J. Cyclam functionalized carbon dots sensor for sensitive and selective detection of copper(II) ion and sulfide anion in aqueous media and its imaging in live cells. *Sens. Actuators B Chem.* **2016**, *224*, 298−306.
(47) Li, C.; Liu, W.; Ren, Y.; Sun, X.; Pan, W.; Wang, J. The selectivity of the carboxylate groups terminated carbon dots switched by buffer solutions for the detection of multi-metal ions. *Sens. Actuators, B Chem.* **2017**, *240*, 941−948.
(48) Chen, Y.; Sun, X.; Pan, W.; Yu, G.; Wang, J. Fe^{3+}-Sensitive Carbon Dots for Detection of Fe^{3+} in Aqueous Solution and Intracellular Imaging of Fe^{3+} Inside Fungal Cells. *Front. Chem.* **2020**, *7*, 911.

https://dx.doi.org/10.1021/acsomega.0c00707
ACS Omega 2020, 5, 7025−7031